Distributed Structures Underlie Gating Differences between the K_{in} Channel KAT1 and the K_{out} Channel SKOR

Janin Riedelsberger[a,b,2], Tripti Sharma[a,b,2], Wendy Gonzalez[c,1,2], Pawel Gajdanowicz[a,2], Samuel Elías Morales-Navarro[c], Carlos Garcia-Mata[d,e], Bernd Mueller-Roeber[b,f], Fernando Danilo González-Nilo[c], Michael R. Blatt[d] and Ingo Dreyer[a,1]

a Universität Potsdam, Institut für Biochemie und Biologie, Molekularbiologie, Heisenberg-Gruppe Biophysik und Molekulare Pflanzenbiologie BPMPB, Karl-Liebknecht-Strasse 24–25, Haus 20, D-14476 Potsdam-Golm, Germany
b Max-Planck Institute of Molecular Plant Physiology, 14476 Potsdam-Golm, Germany
c Centro de Bioinformática y Simulación Molecular, Universidad de Talca, Casilla 721, Talca, Chile
d Laboratory of Plant Physiology and Biophysics, IBLS Plant Sciences, Bower Building, University of Glasgow, Glasgow G12 8QQ, UK
e Laboratorio de Fisiologia Molecular e Integrativa, Institutos de Investigaciones Biologicas, Universidad Nacional de Mar del Plata, 7600 Mar del Plata Buenos Aires, Argentina
f Universität Potsdam, Institut für Biochemie und Biologie, Abteilung Molekularbiologie, 14476 Potsdam-Golm, Germany

ABSTRACT   The family of voltage-gated (*Shaker*-like) potassium channels in plants includes both inward-rectifying (K_{in}) channels that allow plant cells to accumulate K^+ and outward-rectifying (K_{out}) channels that mediate K^+ efflux. Despite their close structural similarities, K_{in} and K_{out} channels differ in their gating sensitivity towards voltage and the extracellular K^+ concentration. We have carried out a systematic program of domain swapping between the K_{out} channel SKOR and the K_{in} channel KAT1 to examine the impacts on gating of the pore regions, the S4, S5, and the S6 helices. We found that, in particular, the N-terminal part of the S5 played a critical role in KAT1 and SKOR gating. Our findings were supported by molecular dynamics of KAT1 and SKOR homology models. *In silico* analysis revealed that during channel opening and closing, displacement of certain residues, especially in the S5 and S6 segments, is more pronounced in KAT1 than in SKOR. From our analysis of the S4–S6 region, we conclude that gating (and K^+-sensing in SKOR) depend on a number of structural elements that are dispersed over this ~145-residue sequence and that these place additional constraints on configurational rearrangement of the channels during gating.

Key words: *Arabidopsis*; K^+ channel; outward rectifier; inward rectifier; channel protein structure; channel protein–cation interaction; gating, K^+-dependent.

INTRODUCTION

Potassium is a key element in the life of plants. It is vital for growth and plays a key role in diverse physiological processes. It is involved in maintaining the stability of proteins, water balance, photosynthesis, membrane, and osmotic potentials, and participates in the control of the ionic balance of the plant cell, the translocation of photosynthates, and the activation of enzymes. Potassium uptake from the soil and its redistribution throughout the plant are accomplished by different families of potassium transporters and channels. These further differentiate in subfamilies with different properties ensuring an appropriate K^+ balance. Much of our present knowledge in the field of potassium uptake and its redistribution centers on voltage-gated K^+ channels, which have been shown to form the major

K^+ conductance in the plasma membrane of several cell types (Lebaudy et al., 2007). The structure of the major family of plant Kv-like, voltage-gated K^+ channels is quite similar to that of their animal relatives. These channels are tetramers,

composed of four α-subunits. Each subunit consists of six transmembrane segments, designated S1–S6, forming the hydrophobic core of the channel. The S4 transmembrane segment incorporates several positively charged amino acids, which contribute to the voltage sensitivity of the channel. A 'reentrant' pore-forming (so-called P) loop, between S5 and S6 controls the passage of ions through the channel and determines its ion selectivity.

In spite of the overall structural similarities, there is enormous functional variety within this family of voltage-gated K$^+$ channels in plants (Gambale and Uozumi, 2006; Dreyer and Blatt, 2009). In the model plant *Arabidopsis thaliana*, the nuclear genome includes a total of nine genes coding for voltage-gated K$^+$ channels. Among those, eight have functionally been characterized. Four of them (*KAT1*, *KAT2*, *AKT1*, and *SPIK*) code for gene products that were shown to expedite the process of K$^+$ uptake, such as into guard cells, root cells, and pollen tubes (Hirsch et al., 1998; Szyroki et al., 2001; Mouline et al., 2002; Lebaudy et al., 2008). These so-called inward-rectifying (K$_{in}$) channels, are closed at positive and moderate negative voltages, and activate only upon significant membrane hyperpolarization. K$_{in}$ channel α-subunits can form heteromeric channels with K$_{silent}$ α-subunits that alone are not capable of forming functional channels (Dreyer et al., 1997; Reintanz et al., 2002; Formentin et al., 2004; Naso et al., 2006; Bregante et al., 2008; Duby et al., 2008; Naso et al., 2009). The silent subunit is modifying K$_{in}$ channel behavior, such as allowing them to cope with very low external K$^+$ concentrations (Geiger et al., 2009). *AtKC1* is the only gene in *Arabidopsis* coding for a K$_{silent}$ subunit. Another gene, *AKT2*, codes for a channel α-subunit that can build channels alone or co-assemble with other K$_{in}$ channel α-subunits. The resulting homo- or heteromeric channels are activated upon membrane hyperpolarization, but are subject to additional post-translational regulation and show a shifting of the activation threshold to very positive voltage values (Dreyer et al., 2001; Michard et al., 2005a, 2005b). These channels are believed to play a role in plant nutrition through the process of phloem (un)loading (Marten et al., 1999; Lacombe et al., 2000; Deeken et al., 2002). Two other genes (*SKOR* and *GORK*) were shown to enable K$^+$ efflux from guard cells during stomatal closure and loading of the xylem tissue from root cells for root-shoot allocation of potassium (Gaymard et al., 1998; Hosy et al., 2003). These so-called outward-rectifying (K$_{out}$) channels are activated upon membrane depolarization. Along with their voltage sensitivity, outwardly rectifying channels are also sensitive towards the external potassium concentration. K$_{out}$ channels open only at membrane voltages positive of the equilibrium potential for potassium, E$_K$, shifting their range of activity to more positive voltages as the external K$^+$ concentration increases (Blatt, 1988; Schroeder, 1988; Blatt and Gradmann, 1997; Wegner and de Boer, 1997). This K$^+$-sensing mechanism ensures that there is only K$^+$ release from these channels, irrespective of the K$^+$ concentration prevailing outside the cell (Johansson et al., 2006).

It appears quite surprising that structurally similar channels belonging to the same family, sharing sequence identity in their core regions of 40% or even higher, show stunning divergence in activation voltage, K$^+$-sensitivity, and rectification properties. Therefore, we chose the K$_{in}$ channel KAT1 and the K$_{out}$ channel SKOR as prototypes and investigated systematically their structural and functional distinctions (Dreyer et al., 2004; Poree et al., 2005; Johansson et al., 2006; Gajdanowicz et al., 2009). In previous studies, we identified regions in the last transmembrane domain S6 that are involved in K$^+$-dependent gating of K$_{out}$ channels. Here, we explore the role of domains beyond S6—including the pore and the voltage-sensor—to assess their contribution to gating in KAT1 and SKOR. Our results highlight the importance of the different sections between S4 and S6 for gating, but also underline further structural dissimilarities between the two K$^+$ channels.

RESULTS AND DISCUSSION

In a previous study (Gajdanowicz et al., 2009), we investigated in detail the role of the last transmembrane domain (S6) in the two K$_{in}$ and K$_{out}$ channel prototypes KAT1 and SKOR. We focused especially on the central and cytoslic parts in S6 (Figure 1, l/m), and were able to show that these two regions influence gating differently in both channels. One important observation was that neither region of the S6 was sufficient to account for all of the gating characteristics associated with the SKOR channel, leaving open a question about the structural determinants
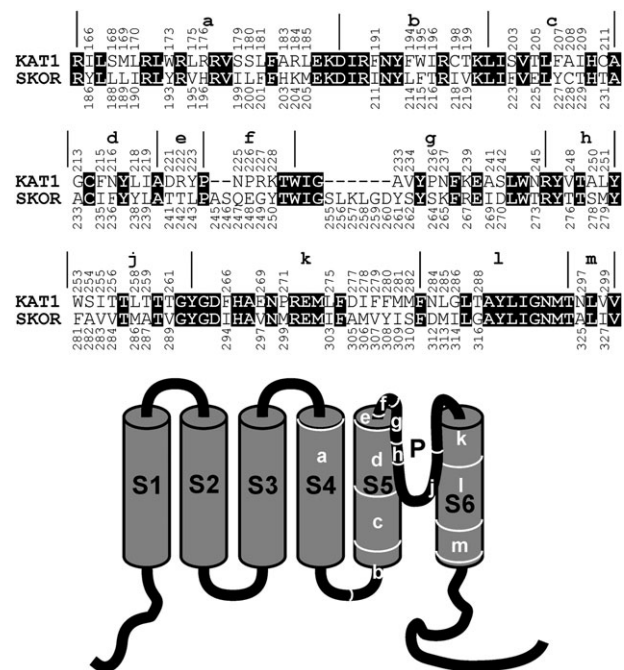

Figure 1. Sequence Comparison of the Region from the S4 to the S6 Domain of the Plant K$_{in}$ Channel KAT1 and the K$_{out}$ Channel SKOR. The regions were subdivided into 12 areas (a/b/c/d/e/f/g/h/j/k/l/m) as indicated.

of gating in this channel. In a search for other regions of plant K⁺ channel proteins contributing to gating, we undertook the construction of KAT1/SKOR chimeras, focusing on domains within the pore region, the S5 helix, and the voltage sensor. The amino acid sequences between transmembrane segments S4 and S6 of KAT1 and SKOR were aligned allowing a subdivision of this part into 12 sections (Figure 1). Based on this partitioning, we undertook a systematic analysis of these domains, carrying out symmetric domain exchanges between the two K⁺ channels, and analyzed the resultant chimeras after heterologous expression in *Xenopus* oocytes.

Pore and S6 Are Not Compatible between KAT1 and SKOR

Key structural determinants important for the K⁺ sensitivity and gating of SKOR are associated with the pore and the S6 helix (Johansson et al., 2006). Therefore, we exchanged the entire P-S6 complex of KAT1 for that of SKOR (Figure 1, h–m). The resulting chimera, however, did not carry any significant current after heterologous expression in *Xenopus* oocytes (Figure 2, KAT1-h-j-k-l-m). Similar negative results were obtained when the pore together with the central and C-terminal regions of the S6 helix were swapped (Figure 2, KAT1-j-l-m), and when the pore along with only the central part of S6 was substituted (Figure 2, KAT1-j-l). Thus, the combined transfer of key residues from the K⁺-sensor of SKOR to KAT1 rendered the channel non-functional instead of introducing a K⁺-sensitivity to KAT1 gating. Nevertheless, replacement of the single regions was tolerated by KAT1. The features of the functional KAT1-l-m channel were already presented elsewhere (Gajdanowicz et al., 2009). Replacing the pore of KAT1
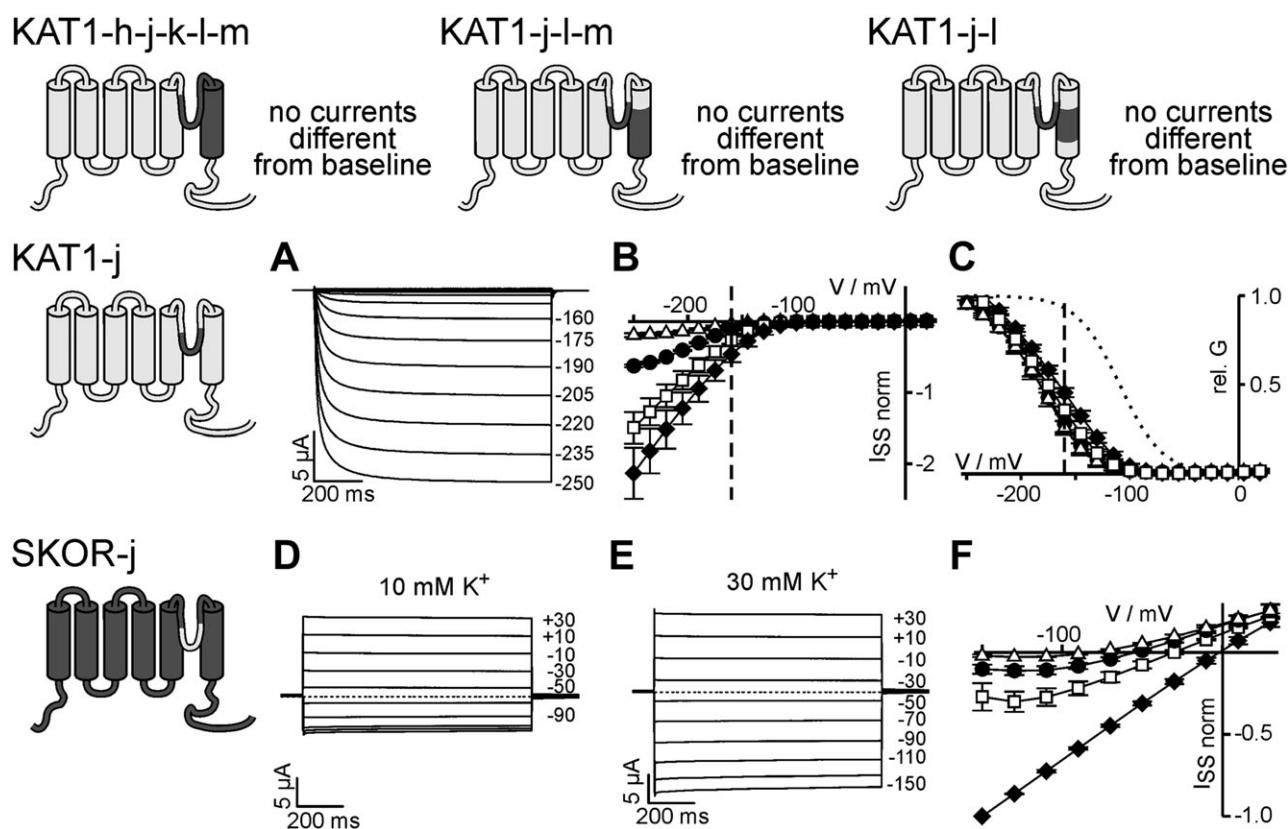

Figure 2. Swapping of the Pore Region Alone or in Combination with Other Domains between the K$_{in}$ Channel KAT1 and the K$_{out}$ Channel SKOR.

Chimeras' structure is indicated and cross-referenced to the regions indicated in Figure 1.

(A–C) Swapping of the pore from SKOR to KAT1 shifts the activation threshold to more negative voltages. Characteristics of the chimera KAT1–j. (A) Representative K⁺ currents recorded in 30 mM K⁺ during 1-s voltage steps from –20 mV to voltages between –250 and +50 mV (15-mV increments) followed by a final step to –60 mV. (B) Steady-state current-voltage curves and (C) relative conductance recorded in 3 (*triangles*), 10 (*circles*), 30 (*squares*), and 100 mM K⁺ (*diamonds*). Data of five cells. Data in (B) were normalized between experiments to values measured in 100 mM K⁺ at –220 mV. The dashed lines in (B) and (C) indicate –160 mV, the most negative voltage usually tested for the KAT1 wild-type and the dotted line in (C) the relative conductance of wild-type KAT1.

(D–F) The chimera SKOR-j is activated by K⁺. (D, E) Representative K⁺ currents of SKOR-j recorded in (D) 10 mM K⁺ and (E) 30 mM K⁺ during 1-s voltage steps from –59 mV (D) and –40 mV (E), respectively, to voltages between –150 and +30 mV (20-mV increments). The dotted lines indicate the zero current. Data are representative for at least three independent experiments. (F) Steady-state current-voltage curves recorded in 3 (*triangles*), 10 (*circles*), 30 (*squares*), and 100 mM K⁺ (*diamonds*). Data of three cells normalized between experiments to values measured in 100 mM K⁺ at –150 mV. In (A), (D), and (E), the step-voltage is indicated in mV for selected traces.

with that of SKOR (KAT1-j) yielded KAT1 channel current, but at voltages displaced approximately –70 mV relative to the wild-type KAT1 (Figure 2, KAT1-j). Similar to the KAT1-l-m chimera, the KAT1-j chimera remained silent over the voltage range from +20 to –130 mV. Current was demonstrable only at more negative voltages (Figure 2A) and was verified by its sensitivity to block by extracellular Cs^{+} (not shown). Otherwise, the KAT1-j current, like that of KAT1, increased in a scalar fashion with [K^{+}]$_o$ (Figure 2B) while the relative conductance (gating) of the channel showed no sensitivity to external K^{+} concentration (Figure 2C). Only the static voltage displacement—and, hence, the energy required to activate the KAT1-j chimera—was increased relative to the wild-type KAT1 K^{+} channel. We quantified the gating of KAT1 and its mutants using a simple two-state model (Michard et al., 2005b). The analysis showed an energy increase of $\Delta (\Delta G) = 3.8 \pm 0.5 \, kT$ for KAT1-j.

The inverse swaps (Figure 1, j and l/m) between KAT1 and SKOR had very different effects on the gating of SKOR. The SKOR K^{+} channel normally rectifies strongly outward, activating on membrane depolarization and in a time- and K^{+}-dependent manner (Figure 3, SKOR). By contrast, both chimeras SKOR-j (Figure 2D–2F) and SKOR-l-m (Gajdanowicz et al., 2009) appeared to be K^{+}-selective leaks without evidence of the kinetic relaxations normally associated with channel (de-)activation (Figure 3, SKOR). These observations indicated that the substitutions greatly reduced the activation energy needed to open the SKOR K^{+} channel. Both substitutions strongly modified the voltage-dependence and inverted the K^{+}-dependence of gating. Whereas a high concentration of external K^{+} suppressed the currents in the wild-type by shifting the activation threshold of the channel to more positive voltage (Johansson et al., 2006), in the two chimeras, it promoted channel activation (Figure 2D–2F). Usually in SKOR, the presence of K^{+} in the pore stabilizes the closed conformation of the channel in such a way that slight changes in the occupancy of the pore are transduced into a modification of the activation energy of this channel. A disruption of this tight connection between the pore and the gating machinery results in a remaining dependency of the pore structure on the external K^{+} concentration as observed also for other open K^{+} channels like, for example, AKT2 (Geiger et al., 2002) or TPK4 (Becker et al., 2004).

Thus, exchanging the corresponding pore or S6 domains of KAT1 and of SKOR had markedly different effects on gating of the two K^{+} channels: whereas the SKOR-j and SKOR-l-m chimeras showed profound and qualitative alterations of the voltage- and K^{+}-dependencies to their gating, the KAT1-j and KAT1-l-m chimeras were affected quantitatively in their gating energy barrier but qualitatively showed all of the gating characteristics of the wild-type channel in relation to extracellular K^{+}.

The Voltage-Sensor of SKOR Is Not Functional in KAT1

Swapping of section 'a', namely the S4 segment, between KAT1 and SKOR resulted in both cases in non-functional channels (Figure 3, KAT1-a and SKOR-a). However, functionality was rescued when, additionally, the motif D-M-I of the S6 gating domain in the SKOR-a chimera was replaced by the KAT1 N-L-G motif. The properties of this SKOR-a-l* chimera (Figure 3) were dominated by the features of the SKOR-D312N-M313L-I314G mutant (Figure 3, SKOR-l*): notably, it was activated by increasing external K^{+} concentrations. Similar results were obtained when the S4-S5 linker (Figure 1, b) of SKOR was replaced by that of KAT1. The chimera SKOR-b was not functional whereas the properties of the functional chimera SKOR-b-l* were dominated by the replacements in the S6 gating domain. In contrast, the exchange of section 'b' in KAT1 by that of SKOR resulted in functional chimeric channels, KAT1-b, showing properties that were not significantly different from those of the KAT1 wild-type. Like KAT1, the chimera KAT1-b was inward-rectifying (Figure 3, KAT1 and KAT1-b) and its gating was not subject to changes in the external K^{+} concentration (not shown). Thus, the voltage-sensor of SKOR was not functional in the KAT1 background and vice versa. In contrast, the S4–S5 linker could be transferred from SKOR to KAT1 (but not from KAT1 to SKOR) without strongly modifying the gating of the channel.

The N-Terminal Part of S5 Plays a Critical Role in SKOR and KAT1

A different picture was drawn from exchanging parts of the S5 region (Figure 1, c–e). The swap of the N-terminal part of S5, section 'c' (Figure 1), was not tolerated either by KAT1 or by SKOR. Even after compensatory mutations of the S6 gating domain, we were unable to rescue channel activity in SKOR (Figure 3, KAT1-c, SKOR-c, SKOR-c-l*). For SKOR, similar results were obtained after exchanging the central part of the S5 segment (Figure 1, d): neither of the chimeras SKOR-d and SKOR-d-l* yielded currents when expressed in *Xenopus* oocytes (Figure 3). In contrast, the reciprocal chimera KAT1-d was a functional inward-rectifying KAT1-like channel (Figure 3, KAT1-d), as was the chimera KAT1-e in which the C-terminal end of S5 was swapped from SKOR to KAT1 (Figure 3, KAT1-e). The inverse exchange from KAT1 to SKOR resulted in non-functional channels (Figure 3, SKOR-e) that could be rescued by additional mutations in the S6 gating domain (Figure 3, SKOR-e-l*). Thus, the S5 segment plays a crucial role in the gating of KAT1 and SKOR. In KAT1, the region could be narrowed down to the N-terminal part of the S5 helix, whereas in SKOR, it extends from the cytosolic end to the central part of S5 helix.

The S5-P linker also proved crucial for function of both K$_{in}$ and K$_{out}$ channels in our hands. The linker between S5 and the pore region (Figure 1, f/g) is the most divergent part in the central cores of SKOR and KAT1. In this area, SKOR comprises, in total, eight additional amino acid residues, two in section 'f' and six in section 'g'. Swapping these sections resulted in non-functional channels in both backgrounds (Figure 3, KAT1-f, SKOR-f, KAT1-g, SKOR-g). Functionality of SKOR-f and SKOR-g could be rescued by additionally exchanging the DMI motif in the S6 gating domain by NLG (Figure 3,
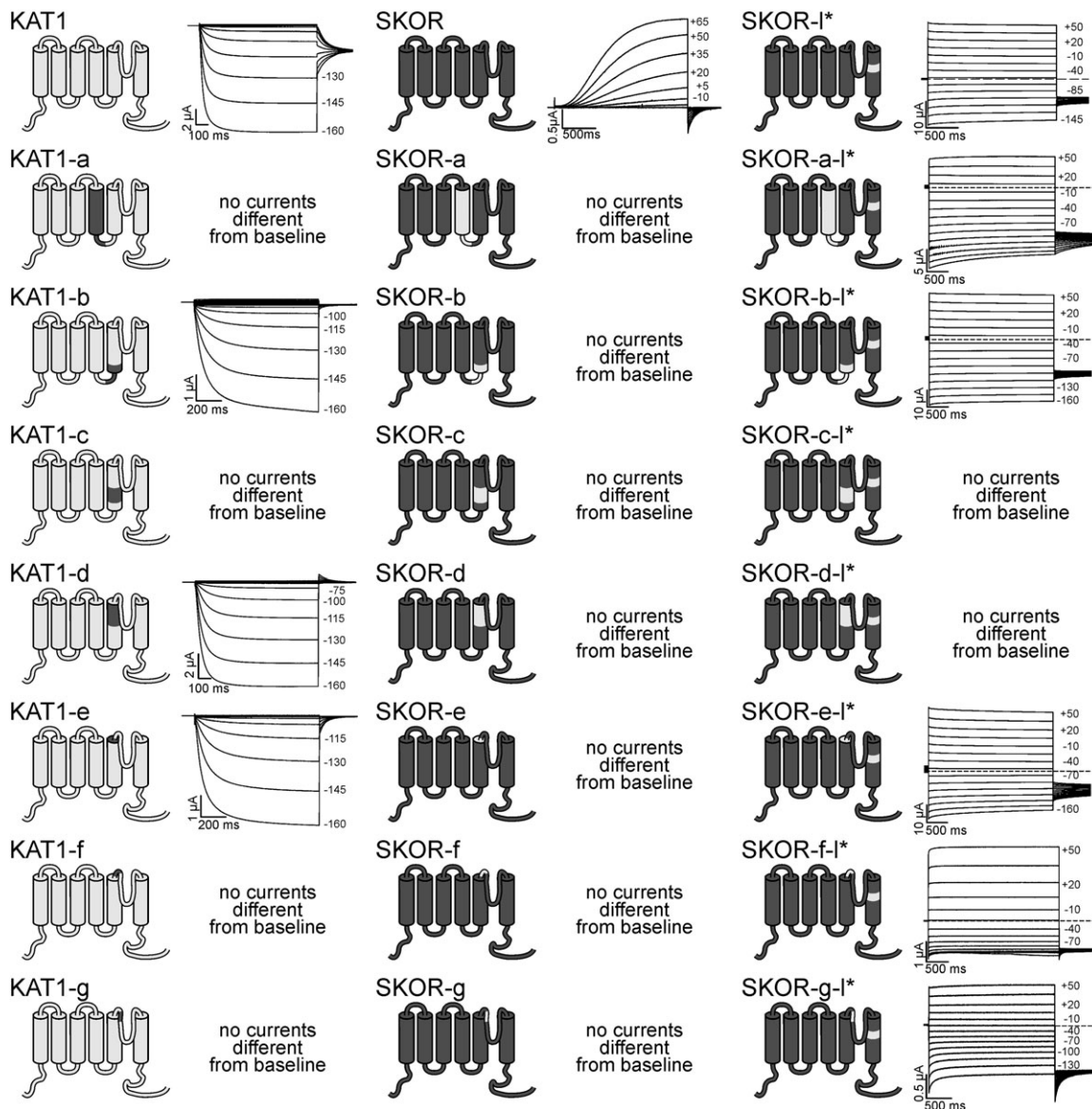
Figure 3. Swapping of Domains between the K_{in} Channel KAT1, the K_{out} Channel SKOR, and the Leak-Like Channel SKOR-D312N-M313L-I314G (= SKOR-l*).

Chimeras' structure is indicated and cross-referenced to the regions indicated in Figure 1. Representative K⁺ currents were recorded in 10 mM K⁺ (KAT1, SKOR, SKOR-l*, KAT1-b, KAT1-d, SKOR-e-l*), 30 mM K⁺ (SKOR-b-l*, KAT1-e, SKOR-f-l*, SKOR-g-l*), and 100 mM K⁺ (SKOR-a-l*). Currents were elicited by voltages between −160 and +50 mV (KAT1, SKOR-a-l*, KAT1-b, SKOR-b-l*, KAT1-d, KAT1-e, SKOR-e-l*, SKOR-f-l*), by voltages between −145 and +50 mV (SKOR-l*, SKOR-g-l*), and by voltages between −85 and +65 mV (SKOR). The dashed lines indicate the zero current level. Displayed data are representative for at least three independent repeats.

SKOR-f-l*, SKOR-g-l*). Thus, we concluded that the S5-P linker is equally important for the different functionalities of KAT1 and SKOR.

Combined Exchanges of Domains Do Not Have Additive Effects

In the SKOR background, the additional exchange of the region l* was able to recover channel activity in five out of the seven tested chimeras—albeit with fundamentally altered properties (Figure 3)—indicating a dominant effect of this S6

gating domain in channel function. Interestingly, in KAT1, such a recovery phenomenon was not observed. Instead, combined domain swaps in the KAT1 background resulted in a heterogeneous picture. Among the 12 segments tested, the exchange of six (b, d, e, j, l, and m) left the KAT1 channel intact. When, for instance, regions j and l were both swapped, channel function could not be detected anymore (Figure 2; KAT1-j-l). In contrast, the chimera KAT1-l-m was functional. It showed properties that were dominated by the KAT1-m exchange (Gajdanowicz et al., 2009). Next, we combined the chimeras KAT1-b, KAT1-d,

KAT1-e, and KAT1-l. All four single chimeras had—also with respect to their activation energy barrier—very similar properties. Nevertheless, the chimeras KAT1-b-d-e-l and KAT1-b-d-e did not carry K$^+$ currents. Only the chimera KAT1-b-d was functional (Figure 4). Thus, in SKOR as well as in KAT1, the effect of multiple domain exchange cannot be predicted by the features of the single exchanges.

Molecular Dynamic Simulations of SKOR and KAT1 Point to Divergences in Gating

Further insights into the gating of KAT1 and SKOR were obtained from analyzing the differences in structural arrangements between the open and the closed states of the two channels. We approximated the channel structures by homology modeling (Gajdanowicz et al., 2009) and compared in molecular dynamics simulations the open and closed state of both channels during equilibration in the membrane. As a measure for structural rearrangements during gating, we calculated the Root Mean Square Deviation (RMSD) for backbone atoms between the open and closed states. Our calculations indicated that structural rearrangements of KAT1 were significantly larger than those of SKOR mainly in the center of the S6 helix (Figure 1, l) and especially at the cytosolic end of S5 (junction between regions b and c), whereas relocations in SKOR appeared to be larger a few amino-acids further downstream in S5 (SKOR-E225, Figure 5). We experimentally assessed this area by generating the mutants SKOR-E225T, SKOR-E225Q, SKOR-C228S, and SKOR-C234S. All four mutants could not be functionally expressed (not shown), supporting the hypothesis that the center of region c plays an important role in SKOR gating. Thus, in a first summary, it can be stated that molecular dynamics simulations pointed to differences in the mobility of certain areas in S5 between KAT1 and SKOR

that may explain the experimentally observed functional incompatibility of these channel regions.

Molecular simulations further revealed valuable insights into the contribution of region l, the S6 gating domain, in channel protein dynamics. Previous studies have shown that this region plays a particular role in K$_{out}$ channel gating (Liu et al., 2005; Poree et al., 2005; Johansson et al., 2006). In the present study, we found additionally in many cases for SKOR that non-functional chimeras could be rescued with further substitutions in region l. To get insights into these features, we modeled the SKOR-l* mutant and compared it with the SKOR wild-type. This analysis revealed that SKOR gating has to be considered as concerted action of the entire channel protein involving inter-subunit interactions rather than independent structural rearrangements of single subunits. In the wild-type channel, region l of one α-subunit interacts in the closed state with region b of the neighboring subunit (Figure 6) while in the open state, it does not. It is therefore tempting to speculate that the inter-subunit interaction between regions l and b might stabilize the closed state of the channel—a hypothesis supported by the model of the SKOR-l* mutant. In this mutant, the l-b interaction got lost in part (Figure 6). Especially the interaction of the S6 gating domain, and here mainly I314, with residues F215, T216, and R217 in region b, was disrupted. As a consequence, the closed state in the SKOR-l* mutant would be destabilized and the channel mutant would stay predominantly in the open configuration. Thus, the molecular dynamics simulations indicate that the loss of interaction between sections l and b might account in the SKOR-l* mutant for the absence of kinetic relaxations normally associated with SKOR channel (de-)activation and for the largely reduced activation energy needed to open the channel as observed earlier (Johansson et al., 2006).
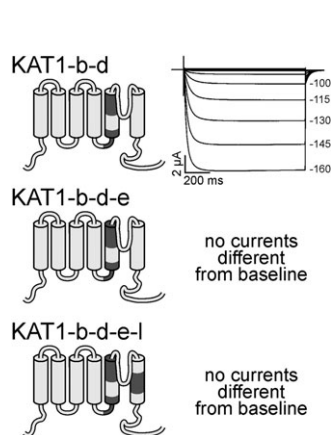

Figure 4. Multiple Domain Swapping Is Only in Part Tolerated by KAT1.

Chimeras' structure is indicated and cross-referenced to the regions indicated in Figure 1. Representative K$^+$ currents of the chimera KAT1-b-d were recorded in 30 mM K$^+$ and elicited by voltages between –160 and +50 mV. Displayed data are representative for at least three independent repeats.
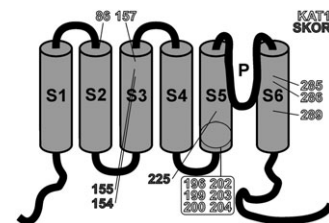

Figure 5. Residues Showing Different Displacements during Gating in SKOR and KAT1.

Numbers in light gray represent the KAT1 amino acids that show a larger displacement in KAT1 than the corresponding residues in SKOR (rmsdSKOR$_{109}$ – rmsdKAT1$_{86}$ = –3.90 Å; rmsdSKOR$_{177}$ – rmsdKAT1$_{157}$ = –2.63 Å; rmsdSKOR$_{196}$ – rmsdKAT1$_{219}$ = –2.33 Å; rmsdSKOR$_{219}$ – rmsdKAT1$_{199}$ = –2.76 Å; rmsdSKOR$_{220}$ – rmsdKAT1$_{200}$ = –5.01 Å; rmsdSKOR$_{222}$ – rmsdKAT1$_{202}$ = –2.07 Å; rmsdSKOR$_{223}$ – rmsdKAT1$_{203}$ = –6.95 Å; rmsdSKOR$_{224}$ – rmsdKAT1$_{204}$ = –2.81 Å; rmsdSKOR$_{313}$ – rmsdKAT1$_{285}$ = –2.09 Å; rmsdSKOR$_{314}$ – rmsdKAT1286 = –1.84 Å; rmsdSKOR$_{317}$ – rmsdKAT1$_{289}$ = –2.37 Å). Dark gray numbers represented the SKOR amino acids that show a larger displacement in SKOR than the corresponding residues in KAT1 (rmsdSKOR$_{174}$ – rmsdKAT1$_{154}$ = 3.41 Å; rmsdSKOR$_{175}$ – rmsdKAT1$_{155}$ = 3.89 Å; rmsdSKOR$_{225}$ – rmsdKAT1$_{205}$ = 3.05 Å).
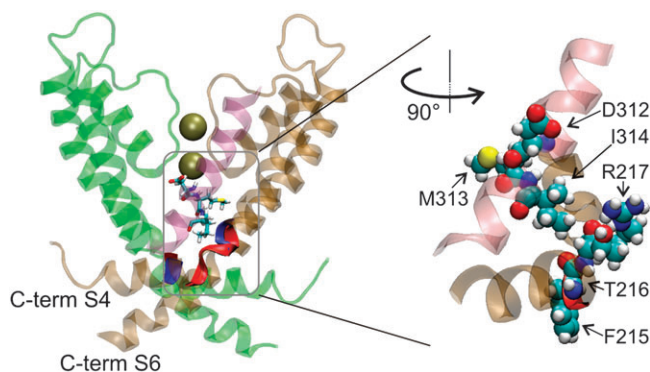
Figure 6. Exchanging the Center of the SKOR-S6 Helix by that of KAT1 Disrupts the Interaction with the S4–S5 Linker in the Closed State.

Left part: For simplicity, only two subunits from the C-terminal end of S4 to the C-terminal end of S6 of a tetrameric SKOR channel are shown (green and brown). The S6 segment of another subunit from residue 300–319 is shown in magenta. The amino acids of the l-region from the magenta subunit are represented in licorice. The stretch in blue indicates the S4–S5 linker zones that interact with region l of the magenta subunit. Zones of the S4–S5 linker from the brown subunit that interact with region l of the magenta subunit in the SKOR wild-type but not with region l* in the SKOR-l* chimera are labeled in red (located in the blue stretch). Right part: Close-up view of the indicated region turned by 90° around the z-axis. Residues D312, M313, I314 of region l and F215, T216, R217 of region b are displayed in Van-der-Waals representation. In the wild-type, I314 is interacting with F215, T216, and R217. In the SKOR-l* chimera, especially residue I314 is replaced by a glycine. As a consequence, the interaction is lost.

The destabilization of the closed state may also provide an explanation for the rescue effect of SKOR-l*. In many cases, additional substitution of region l* could rescue non-functional chimeras (e.g. SKOR-a, SKOR-b, SKOR-e, SKOR-f, SKOR-g). However, for SKOR-c and SKOR-d, this strategy failed. The chimeras SKOR-c-l* and SKOR-d-l* remained non-functional, indicating that either the closed-state destabilization was not sufficient in these cases or replacement of regions c and d are structurally not tolerated by other channel parts. Modeling of SKOR (Figure 7A) and KAT1 (not shown) supports the conclusion that compatible S6-P-S5 residue clusters are important for proper channel function by forming inter- and intra-subunit connections. Region d, for instance, borders on regions c, e, j, and k. Likewise, region c interacts with regions b, d, j, k, and l of the same subunit but, interestingly, also with region k of the neighboring subunit (Figure 7B). Thus, especially region c plays a central role in connecting different parts of the channel protein that are important for gating. As pointed out before, the functionality of this section slightly differs between KAT1 and SKOR, suggesting that the N-terminal part of S5 is one key element for discriminating K_{in} and K_{out} channel gating.

This conclusion is further supported by independent approaches. For instance, Li et al. (2008) generated a nonfunctional chimera between the S5-P-S6 regions of the inward-
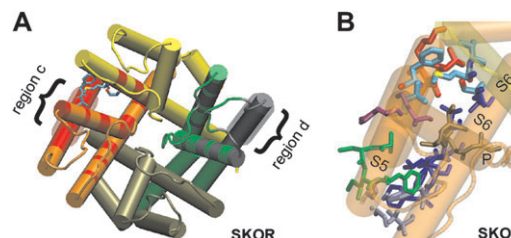

Figure 7. Model of SKOR in the Open State to Illustrate Interacting Zones.

(A) Look on the SKOR channel from the extracellular side. The different subunits are represented in orange, yellow, green, and metal, respectively. The region c is explicitly displayed only in the orange subunit and region d only in the green subunit. Interacting zones of region c are regions b, d, j, k, and l of the same subunit (represented in red in the orange subunit), and region k of the neighboring subunit (red marks in the yellow subunit). The specific residues that interact between region c of the orange subunit and region k of the yellow subunit are: F223 and L226 with M306, V307, and S310 (represented in licorice). Interacting zones of region d are regions c, e, j, and k of the same subunit (gray).
(B) Close-up view on residues interacting with region c. Interacting zones of region c are regions b (red, residues I218 to K220), d (green, residues A233 to F236), h (purple, residues Y275 and M279), j (brown, residues A282, V283, M286, A287), k of same subunit (orange; residues in iceblue, F304, Y308), l (blue, residues F311, D312, L315, G316, Y318, L319, M323), and region k of the neighboring subunit (yellow). The specific residues that interact between region c of the orange subunit and region k of the yellow subunit (F223 and L226 with M306, V307, and S310) are represented by colors assigned for each atom in VMD.

rectifying K⁺ channel LKT1 (i.e. regions c–l) and the rest of SKOR. Functionality of this chimera could be rescued in a random mutagenesis approach by additional mutations in region c, particularly at the position equivalent to SKOR-E225 (Figure 5). Interestingly, some of the rescued mutants were similar to the leak-like chimeras SKOR-a-l*, SKOR-b-l*, SKOR-e-l*, SKOR-f-l*, SKOR-g-l*, whereas others showed additional signs of hyperpolarization activation.

For KAT1, it was already shown that the S5 domain closely interacts with the voltage-sensor S4, too (Lai et al., 2005). Therefore, not only matching S5-P-S6 pairs are important for proper channel function, but also matching S4–S5 pairs. On these grounds, it is now comprehensible that the voltage-sensor of SKOR was not functional in KAT1; albeit the charged residues, and therefore those residues that drive the movement of this segment during voltage-gating (Latorre et al., 2003a, 2003b), are almost identical. Despite the common charge environment, at other positions, the S4 segments differ. Single domain swaps may therefore distort the tight balance of the channel's 3D-puzzle and only the simultaneous exchange of two, three, or more matching regions would maintain channel functionality.

Conclusion

Gating of K_{in} and K_{out} channels, represented by KAT1 and SKOR, shares an extensive structural background, but leads

to profoundly different biophysical characteristics. In this study, we investigated 12 regions in the S4–S6 domains of SKOR and KAT1 by analyzing 37 chimeras. Although this subset represents only 0.9% of all possible 2^{12} combinations, we find that gating (and K+-sensing in SKOR) depend on a number of structural elements that are dispersed over this 145-residue sequence. One key element for discriminating K_{in} and K_{out} channel gating appears to be the N-terminal part of the S5 transmembrane helix.

METHODS

Molecular Genetics and Expression

SKOR and KAT1 mutation, expression, and analysis used standard molecular genetic methods. Site mutations and chimera constructs were generated as described previously (Poree et al., 2005; Johansson et al., 2006). All mutants were verified by sequencing. For expression, the coding regions of wild-type and mutant channels were cloned into the vector pGEMHE and cRNA was synthesized using T7 polymerase (mMessage mMachine, Ambion Europe Ltd, Huntingdon, UK). For expression in oocytes, stage V and VI oocytes were taken from *Xenopus laevis* and maintained at 18°C in a modified Barth's medium containing 96 mM NaCl, 2 mM KCl, 1 mM CaCl$_2$, 1 mM MgCl$_2$, and 10 mM HEPES/NaOH (pH 7.4). Oocytes were defolliculated by collagenase treatment (2 mg ml^{-1}, type IA, No. C9891, Sigma, Taufkirchen, Germany). Defolliculated oocytes were injected with 40 ng (1 μg μl^{-1}) cRNA using a solid displacement injector (Picospritzer III, Parker Instrumentation, Fairfield, NJ, USA) and kept at 18–20°C. Control oocytes were injected with 40 nl of deionized water.

Electrophysiology

Whole-cell currents were measured under voltage clamp (Turbo TEC-10CX; NPI Electronic, Tamm, Germany) with a two-electrode clamp circuit and virtual ground. Voltage control, data acquisition, and data analyses were carried out using the Pulse/PulseFit software (HEKA, Lambrecht/Pfalz, Germany). Measurements were performed in bath solutions containing 1 mM CaCl$_2$ and 2 mM MgCl$_2$, buffered with 10 mM Tris/MES, pH 7.4, with the addition of K3: 3 mM KCl and 97 mM NaCl; K10: 10 mM KCl and 90 mM NaCl; K30: 30 mM KCl and 70 mM NaCl; K100: 100 mM KCl. Measurements were repeated routinely at the end of each treatment with the addition of 10 mM CsCl to distinguish K+ currents and any background, non-selective leak. In experiments testing very negative voltages (less than –170 mV), 1 mM LaCl$_3$ was added to the bath solution to efficiently suppress possible endogenous currents at these voltages (Naso et al., 2006).

Data Analysis

To standardize comparisons of wild-type with mutant channel currents, relative conductances were obtained in two-step pulse experiments. In a first pulse (variable voltage *V*), channels were activated followed by a tail-pulse (non-variable voltage V_T). The current measured at the end of the first pulse is the steady-state current I_{SS}. The current measured at the onset of the tail-pulse, tail current I_T, can be expressed as $I_T(V) = N \times i(V_T) \times P_{open}(V)$, where $P_{open}(V)$ is the open probability of the channel at the end of the first pulse. Thus, the tail current is proportional to the open probability $P_{open}(V)$. The resulting curves were fitted such that:

$$I_T(V) = I_{max}/\left[1 + \exp\left(-(V - V_{1/2})/V_S\right)\right] + \text{offset},$$
$$\text{(Equation 1)}$$

where I_{max} is the maximum current, *V* is the voltage of the activation pulse, $V_{1/2}$ is the voltage giving half-maximal conductance, V_S is the voltage sensitivity coefficient, the parameter offset is a constant. Fittings were carried out using a Marquardt–Levenberg algorithm (Marquardt, 1963) and the resulting values for I_{max} and offset used to calculate relative conductances rel.$G = [I_T(V) - \text{offset}]/I_{max}$. Current records were corrected for background current, estimated as a linear leak component from measurements between –130 and –160 mV after substituting Cs+ for K+ to block the K+ channels. Measurements were discarded when the maximum leak current exceeded 5% of the maximum current in the steady state. To describe gating with a two-state model (Michard et al., 2005b) and to quantify the energy difference between open and closed state, ΔG_{OC}, a Boltzmann function was fitted to the rel.$G(V)$ values:

$$\text{rel}.G(V) = \frac{1}{1 + e^{-\left(\frac{\Delta G_{OC}}{kT}\right)}} = \frac{1}{1 + e^{-z\frac{e_0}{kT}(V - V_{1/2})}} \quad \text{(Equation 2)}$$

resulting in $\Delta G_{OC} = z \times e_0 \times (V - V_{1/2})$ values that could be compared as $\Delta(\Delta G) = \Delta G_{OC}^{mutant} - \Delta G_{OC}^{wild-type}$. *z* is the apparent gating charge, e_0 is the elementary charge, and *k* and *T* have their usual meanings. To reduce the number of free parameters, fits were constrained by the adjustment of a common value *z* for all KAT1-based and SKOR-based datasets, respectively. Results are reported as means ± standard deviation where appropriate.

Analysis for KAT1 and SKOR Molecular Dynamics

KAT1 and SKOR homology models (in open and closed state) were built on the basis of the Kv1.2 model obtained by the Rosseta method (Yarov-Yarovoy et al., 2006) and optimized using energy minimization. Minimization was followed by an equilibration step using a molecular dynamics (MD) simulation in membrane for 1 ns (Gajdanowicz et al., 2009). Structures of the protein were saved every 10 ps from the MD trajectory for analysis. Structural rearrangements between open and closed state trajectories were compared using Root Mean Square Deviation (RMSD). RMSD for all backbone atoms was calculated with an in-house script for the VMD program (Humphrey et al., 1996). Before RMSD calculation, the protein backbone of the open state was aligned with that of the closed state. Differences in structural rearrangements between SKOR

and KAT1 were calculated for each amino acid on the basis of a previous SKOR–KAT1 alignment (Poree et al., 2005) as rmsdSKOR$_{aax}$ – rmsdKAT1$_{aay}$, where rmsdSKOR$_{aax}$ denotes the RMSD of amino acid SKOR-x from the open to the closed state and rmsdKAT1$_{aay}$ the RMSD of the corresponding amino acid KAT1-y. As a threshold to assign a difference as significant, we chose a value of 2 Å (Carugo, 2007).

Molecular Model for the SKOR-l* Mutant

The chimera SKOR-l* (= SKOR-D312N-M313L-I314G) was built *in silico* in the open and the closed state. SKOR-l* was built using the plug-in *mutate* of the VMD program on the basis of the homology models of the SKOR wild-type in the open and closed states. The SKOR-l* mutant was inserted into the membrane, minimized and equilibrated following the same protocol as applied for wild-type SKOR (Gajdanowicz et al., 2009).

REFERENCES

Becker, D., et al. (2004). AtTPK4, an *Arabidopsis* tandem-pore K$^+$ channel, poised to control the pollen membrane voltage in a pH- and Ca^{2+}-dependent manner. Proc. Natl Acad. Sci. U S A. **101,** 15621–15626.

Blatt, M.R. (1988). Potassium-dependent bipolar gating of potassium channels in guard cells. J. Membr. Biol. **102,** 235–246.

Blatt, M.R., and Gradmann, D. (1997). K$^+$-sensitive gating of the K$^+$ outward rectifier in *Vicia* guard cells. J. Membr. Biol. **158,** 241–256.

Bregante, M., Yang, Y., Formentin, E., Carpaneto, A., Schroeder, J.I., Gambale, F., Lo, S.F., and Costa, A. (2008). KDC1, a carrot Shaker-like potassium channel, reveals its role as a silent regulatory subunit when expressed in plant cells. Plant Mol. Biol. **66,** 61–72.

Carugo, O. (2007). Statistical validation of the root-mean-square-distance, a measure of protein structural proximity. Protein Eng. Des.Sel. **20,** 33–37.

Deeken, R., Geiger, D., Fromm, J., Koroleva, O., Ache, P., Langenfeld-Heyser, R., Sauer, N., May, S.T., and Hedrich, R. (2002). Loss of the AKT2/3 potassium channel affects sugar loading into the phloem of *Arabidopsis*. Planta. **216,** 334–344.

Dreyer, I., and Blatt, M.R. (2009). What makes a gate? The ins and outs of Kv-like K$^+$ channels in plants. Trends Plant Sci. **14,** 383–390.

Dreyer, I., Antunes, S., Hoshi, T., Mueller-Roeber, B., Palme, K., Pongs, O., Reintanz, B., and Hedrich, R. (1997). Plant K$^+$ channel alpha-subunits assemble indiscriminately. Biophys.J. **72,** 2143–2150.

Dreyer, I., Michard, E., Lacombe, B., and Thibaud, J.B. (2001). A plant Shaker-like K$^+$ channel switches between two distinct gating modes resulting in either inward-rectifying or 'leak' current. FEBS Lett. **505,** 233–239.

Dreyer, I., Poree, F., Schneider, A., Mittelstädt, J., Bertl, A., Sentenac, H., Thibaud, J.B., and Mueller-Roeber, B. (2004). Assembly of plant *Shaker*-like Kout channels requires two distinct sites of the channel alpha-subunit. Biophys. J. **87,** 858–872.

Duby, G., Hosy, E., Fizames, C., Alcon, C., Costa, A., Sentenac, H., and Thibaud, J.B. (2008). AtKC1, a conditionally targeted Shaker-type subunit, regulates the activity of plant K$^+$ channels. Plant J. **53,** 115–123.

Formentin, E., Varotto, S., Costa, A., Downey, P., Bregante, M., Naso, A., Picco, C., Gambale, F., and LoSchiavo, F. (2004). DKT1, a novel K$^+$ channel from carrot, forms functional heteromeric channels with KDC1. FEBS Lett. **573,** 61–67.

Gajdanowicz, P., Garcia-Mata, C., Gonzalez, W., Morales-Navarro, S.E., Sharma, T., Gonzalez-Nilo, F.D., Gutowicz, J., Mueller-Roeber, B., Blatt, M.R., and Dreyer, I. (2009). Distinct roles of the last transmembrane domain in controlling *Arabidopsis* K$^+$ channel activity. New Phytol. **182,** 380–391.

Gambale, F., and Uozumi, N. (2006). Properties of shaker-type potassium channels in higher plants. J. Membr. Biol. **210,** 1–19.

Gaymard, F., Pilot, G., Lacombe, B., Bouchez, D., Bruneau, D., Boucherez, J., Michaux-Ferriere, N., Thibaud, J.B., and Sentenac, H. (1998). Identification and disruption of a plant shaker-like outward channel involved in K$^+$ release into the xylem sap. Cell. **94,** 647–655.

Geiger, D., Becker, D., Lacombe, B., and Hedrich, R. (2002). Outer pore residues control the H$^+$ and K$^+$ sensitivity of the *Arabidopsis* potassium channel AKT3. Plant Cell. **14,** 1859–1868.

Geiger, D., Becker, D., Vosloh, D., Gambale, F., Palme, K., Rehers, M., Anschuetz, U., Dreyer, I., Kudla, J., and Hedrich, R. (2009). Heteromeric AtKC1/AKT1 channels in *Arabidopsis* roots facilitate growth under K$^+$-limiting conditions. J. Biol. Chem. **284,** 21288–21295.

Hirsch, R.E., Lewis, B.D., Spalding, E.P., and Sussman, M.R. (1998). A role for the AKT1 potassium channel in plant nutrition. Science. **280,** 918–921.

Hosy, E., et al. (2003). The *Arabidopsis* outward K$^+$ channel GORK is involved in regulation of stomatal movements and plant transpiration. Proc. Natl Acad. Sci. U S A. **100,** 5549–5554.

Humphrey, W., Dalke, A., and Schulten, K. (1996). VMD: visual molecular dynamics. J. Mol. Graph. **14,** 33–38.

Johansson, I., et al. (2006). External K$^+$ modulates the activity of the *Arabidopsis* potassium channel SKOR via an unusual mechanism. Plant J. **46,** 269–281.

Lacombe, B., Pilot, G., Michard, E., Gaymard, F., Sentenac, H., and Thibaud, J.B. (2000). A *Shaker*-like K⁺ channel with weak rectification is expressed in both source and sink phloem tissues of *Arabidopsis*. Plant Cell. **12,** 837–851.

Lai, H.C., Grabe, M., Jan, Y.N., and Jan, L.Y. (2005). The S4 voltage sensor packs against the pore domain in the KAT1 voltage-gated potassium channel. Neuron. **47,** 395–406.

Latorre, R., Munoz, F., Gozalez, C., and Cosmelli, D. (2003a). Structure and function of potassium channels in plants: some inferences about the molecular origin of inward rectification in KAT1 channels. Mol. Membr. Biol. **20,** 19–25.

Latorre, R., Olcese, R., Basso, C., Gonzalez, C., Munoz, F., Cosmelli, D., and Alvarez, O. (2003b). Molecular coupling between voltage sensor and pore opening in the *Arabidopsis* inward rectifier K⁺ channel KAT1. J. Gen. Physiol. **122,** 459–469.

Lebaudy, A., Vavasseur, A., Hosy, E., Dreyer, I., Leonhardt, N., Thibaud, J.B., Very, A.A., Simonneau, T., and Sentenac, H. (2008). Plant adaptation to fluctuating environment and biomass production are strongly dependent on guard cell potassium channels. Proc. Natl Acad. Sci. U S A. **105,** 5271–5276.

Lebaudy, A., Very, A.A., and Sentenac, H. (2007). K⁺ channel activity in plants: genes, regulations and functions. FEBS Lett. **581,** 2357–2366.

Li, L., Liu, K., Hu, Y., Li, D., and Luan, S. (2008). Single mutations convert an outward K⁺ channel into an inward K⁺ channel. Proc. Natl Acad. Sci. U S A. **105,** 2871–2876.

Liu, K., Li, L., and Luan, S. (2005). An essential function of phosphatidylinositol phosphates in activation of plant shaker-type K⁺ channels. Plant J. **42,** 433–443.

Marquardt, D.W. (1963). An algorithm for least squares estimation of nonlinear parameters. J. Soc. Ind. Appl. Math. **11,** 431–441.

Marten, I., Hoth, S., Deeken, R., Ache, P., Ketchum, K.A., Hoshi, T., and Hedrich, R. (1999). AKT3, a phloem-localized K⁺ channel, is blocked by protons. Proc. Natl Acad. Sci. U S A. **96,** 7581–7586.

Michard, E., Dreyer, I., Lacombe, B., Sentenac, H., and Thibaud, J.B. (2005a). Inward rectification of the AKT2 channel abolished by voltage-dependent phosphorylation. Plant J. **44,** 783–797.

Michard, E., Lacombe, B., Poree, F., Mueller-Roeber, B., Sentenac, H., Thibaud, J.B., and Dreyer, I. (2005b). A unique voltage sensor sensitizes the potassium channel AKT2 to phosphoregulation. J. Gen. Physiol. **126,** 605–617.

Mouline, K., Very, A.A., Gaymard, F., Boucherez, J., Pilot, G., Devic, M., Bouchez, D., Thibaud, J.B., and Sentenac, H. (2002). Pollen tube development and competitive ability are impaired by disruption of a Shaker K⁺ channel in *Arabidopsis*. Genes Dev. **16,** 339–350.

Naso, A., Dreyer, I., Pedemonte, L., Testa, I., Gomez-Porras, J.L., Usai, C., Mueller-Rueber, B., Diaspro, A., Gambale, F., and Picco, C. (2009). The role of the C-terminus for functional heteromerization of the plant channel KDC1. Biophys. J. **96,** 4063–4074.

Naso, A., Montisci, R., Gambale, F., and Picco, C. (2006). Stoichiometry studies reveal functional properties of KDC1 in plant shaker potassium channels. Biophys. J. **91,** 3673–3683.

Poree, F., Wulfetange, K., Naso, A., Carpaneto, A., Roller, A., Natura, G., Bertl, A., Sentenac, H., Thibaud, J.B., and Dreyer, I. (2005). Plant K_{in} and K_{out} channels: approaching the trait of opposite rectification by analyzing more than 250 KAT1-SKOR chimeras. Biochem. Biophys. Res. Commun. **332,** 465–473.

Reintanz, B., Szyroki, A., Ivashikina, N., Ache, P., Godde, M., Becker, D., Palme, K., and Hedrich, R. (2002). AtKC1, a silent *Arabidopsis* potassium channel alpha-subunit modulates root hair K⁺ influx. Proc. Natl Acad. Sci. U S A. **99,** 4079–4084.

Schroeder, J.I. (1988). K⁺ transport properties of K⁺ channels in the plasma membrane of *Vicia faba* guard cells. J. Gen. Physiol. **92,** 667–683.

Szyroki, A., et al. (2001). KAT1 is not essential for stomatal opening. Proc. Natl Acad. Sci. U S A. **98,** 2917–2921.

Wegner, L.H., and de Boer, A.H. (1997). Properties of two outward-rectifying channels in root xylem parenchyma cells suggest a role in K⁺ homeostasis and long- distance signaling. Plant Physiol. **115,** 1707–1719.

Yarov-Yarovoy, V., Baker, D., and Catterall, W.A. (2006). Voltage sensor conformations in the open and closed states in ROSETTA structural models of K⁺ channels. Proc. Natl Acad. Sci. U S A. **103,** 7292–7297.